Food Hydrocolloids 127 (2022) 107510

Contents lists available at ScienceDirect

Food Hydrocolloids

journal homepage: www.elsevier.com/locate/foodhyd

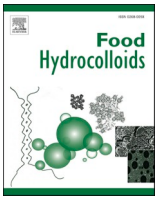

Inter-laboratory analysis of cereal beta-glucan extracts of nutritional importance: An evaluation of different methods for determining weight-average molecular weight and molecular weight distribution

Simon Ballance [a,*], Yudong Lu [b], Hanne Zobel [a], Anne Rieder [a], Svein Halvor Knutsen [a], Vlad T. Dinu [b], Bjørn E. Christensen [c], Ann-Sissel Ulset [c], Marius Schmid [d], Ndegwa Maina [e], Antje Potthast [f], Sonja Schiehser [f], Peter R. Ellis [g], Stephen E. Harding [b,h]

[a] Nofima AS - Norwegian Institute of Food, Fisheries and Aquaculture Research, PB 210, NO, 1431, Norway
[b] National Centre for Macromolecular Hydrodynamics (NCMH), University of Nottingham, School of Biosciences, Sutton Bonington, LE12 5RD, UK
[c] Department of Biotechnology and Food Science, NTNU, Trondheim, Norway
[d] ZentriForce Pharma Research GmbH, Heidelberg, Germany
[e] Department of Food and Nutrition, University of Helsinki, Helsinki, Finland
[f] Institute of Chemistry of Renewable Resources, University of Natural Resources and Life Sciences (BOKU), Muthgasse 18, A-1190, Vienna, Austria
[g] Biopolymers Group, Departments of Biochemistry and Nutritional Sciences, Faculty of Life Sciences and Medicine, King's College London, Franklin-Wilkins Building, 150 Stamford Street, London, SE1 9NH, UK
[h] KHM, University of Oslo, Postboks 6762, St. Olavs Plass, 0130, Oslo, Norway

ARTICLE INFO

Keywords:
Dietary fibre
Light scattering
Molar mass
Molecules
Aggregates

ABSTRACT

In an interlaboratory study we compare different methods to determine the weight-average molecular weight (M_w) and molecular weight distribution of six cereal beta-glucan isolates of nutritional importance. Size-exclusion chromatography (SEC) with multi-angle light scattering (MALS), capillary viscometry, sedimentation velocity analytical ultracentrifugation and one asymmetric flow field-flow fractionation (AF4)-MALS method all yielded similar M_w values for mostly individual chains of dissolved beta-glucan molecules. SEC with post-column calcofluor detection underestimated the M_w of beta-glucan >500 × 10^3 g/mol. The beta-glucan molecules analysed by these methods were primarily in a random coil conformation as evidenced from individual Mark-Houwink-Kuhn-Sakurada (MHKS) scaling coefficients between 0.5 and 0.6 and Wales-Van Holde ratios between 1.4 and 1.7. In contrast, a second AF4-MALS method yielded much larger M_w values for these same samples indicating the presence and detection of beta-glucan aggregates. Storage of the six beta-glucan solutions in the dark at 4 °C for 4 years revealed them to be stable. This suggests an absence of storage-induced irreversible aggregation phenomena or chain-scission. Shear forces in SEC and the viscometer capillary and hydrostatic pressure in analytical ultracentrifugation probably led to the reversable dissociation of beta-glucan aggregates into molecularly dissolved species. Thus, all these methods yield true weight-average molecular weight values not biased by the presence of aggregates as was the case in one of the AF4 based methods employed.

1. Introduction

Oat and barley 1,3, 1,4-β-D-glucans (BG) are dietary fibres with positive health benefits endorsed by the European Food Safety Authority (EFSA) and U.S. Food and Drug Administration (FDA). These benefits include a capacity to lower fasting blood cholesterol and attenuate post-prandial glycaemic responses (EFSA, 2010; 2011a; 2011b). These metabolic effects have been attributed to the molecular weight (*M*) of dietary BG along with their extractability/solubility and consequent dissolved concentration in the upper gastrointestinal tract (Grundy et al., 2017; Rieder, Knutsen, & Ballance, 2017). It has been shown that hydrated BG of high *M,* which can generate high levels of viscosity, tend to be the most physiologically effective (Brummer, Duss, Wolever, & Tosh, 2012; Regand, Tosh, Wolever, & Wood, 2009; Rieder et al., 2017; Tosh, Brummer, Wolever, & Wood, 2008; Wang et al., 2015; Wolever et al., 2010b). For instance, mechanistic studies have indicated that the

* Corresponding author. Nofima AS Norwegian Institute of Food, Fisheries, and Aquaculture Research Osloveien, 1 1433 Ås, Norway.
E-mail address: simon.ballance@nofima.no (S. Ballance).

https://doi.org/10.1016/j.foodhyd.2022.107510
Received 19 November 2021; Received in revised form 13 January 2022; Accepted 15 January 2022
Available online 20 January 2022

retention of high *M* in BG is important in reducing postprandial glycaemia and insulinaemia. This metabolic effect seems to be linked to a decrease in the rate of starch digestion and glucose absorption caused by an increase in digesta viscosity in the proximal gut (Wang & Ellis, 2014). Other physiological mechanisms of BG that may also have an impact include delayed gastric emptying (Thondre, Shafat, & Clegg, 2013), direct inhibition of α-amylase activity (Xiao et al., 2020), and a decrease in the nutrient permeability of the intestinal mucus layer (Mackie, Rigby, Harvey, & Bajka, 2016). Another area of interest in the *M* of BG is associated with brewing where barley BG may cause filtration difficulties during malting and mashing (Jin, Speers, Paulson, & Stewart, 2004).

Over the years many different methods, employed by a plethora of researchers working in different laboratories, have been applied to determine *M* characteristics of BG, which requires sources of BG extracts (Lazaridou, Biliaderis, & Izydorczyk, 2007). Thus, the measured *M* characteristics of BG are not only a function of their origin, such as the pure polymer standards or extracts of different oat and barley containing foods and ingredients, but also of the extraction or solubilisation procedure, which can for example lead to depolymerisation (Rimsten, Stenberg, Andersson, Andersson, & Åman, 2003), and the analytical method that is employed. The huge differences in *M* reported for BG from 2000 g/mol to 40 × 10^6 g/mol (Grimm et al., 1995) are therefore not surprising. Even for high purity, and identical samples, literature *M* values vary by orders of magnitude depending on methods used for dissolution, sample preparation, and measurement. Values are quoted for beta-glucan preparations that comprise different amounts of single molecules, aggregates, and supramolecular aggregates including dispersions of essentially undissolved material. For example, weight average molecular weight (M_w) values for a commercially available barley beta-glucan standard (Megazyme), analysed by size-exclusion chromatography-light scattering-refractive index detection (SEC-LS-RI), have been quoted at 359000 g/mol dissolved in 0.05 M NaOH (product datasheet) and 520000 g/mol when dissolved in 0.01 M LiBr/DMSO (Mäkelä, Sontag-Strohm, & Maina, 2015). Both these estimates were determined presumably on solutions of single molecules. The same sample analysed with asymmetric flow field-flow fractionation-multi-angle light scattering (AF4-MALS) coupled with on-line RI, however, produced a value of 2.8 × 10^6 (Ulmius, Önning, & Nilsson, 2012), presumably comprising both single molecules and aggregates. High standard deviations of M_w between independent replicates (n = 4) of this same sample dissolved in $NaNO_3$ and analysed by AF4-MALS-RI were found with M_w values ranging from 2.0 to 3.7 × 10^6 g/mol (Ulmius et al., 2012). Similar findings with high standard deviations have been reported by using SEC-MALS-RI for samples (n = 3) containing aggregates, likely due to incomplete dissolution of the BG (Wang, Wood, & Cui, 2002). In contrast, relatively similar results for M_w were obtained in an inter-laboratory study of three BG analysed by SEC with different column and detector systems (low and multi-angle light scattering and viscometry) and different dissolution conditions and data processing methods (Christensen et al., 2001). Another inter-laboratory study showed that similar results for apparent *M* characteristics of BG can be obtained with different variants of SEC-post column calcofluor addition and fluorescence detection (SEC-FL) of the BG-calcofluor complex for the same standard solutions of BG using identical calibration standards (Rieder et al., 2015). However, the calcofluor method was shown to underestimate M_w values above 500 × 10^3 g/mol, while the molecular weight at peak (M_p) was identical with values obtained with other detector systems (RI, LS) (Rieder et al., 2015).

It has been known for some decades that cereal BG have a propensity to aggregate in dilute aqueous solutions (pure water, 0.1 M NaCl) and even in chaotropic agents and polar aprotic solvents such as guanidinium hydrochloride, urea, and DMSO (Gómez, Navarro, Manzanares, Horta, & Carbonell, 1997; Grimm, Krüger, & Burchard, 1995; Li, Cui, Wang, & Yada, 2011; Vårum, Smidsrød, & Brant, 1992). In the earliest studies, batch mode multi-angle static light scattering was used to construct a Zimm plot and thus determine M_w. Beta-glucans in a serial dilution series, of which 0.2–2 mg/mL was typical, were characterised including M_w. In many instances, slightly negative second virial coefficient (A_2) values were observed which indicates concentration-dependent aggregation. A downward curvature was also often seen at low scattering angles preventing accurate extrapolation to zero angle to calculate M_w (Li, Wang, Cui, Huang, & Kakuda, 2006). Dynamic light scattering has also been used to detect aggregates (Li et al., 2011; Li et al., 2006). In recent years, AF4 has emerged as a method to separate BG in dilute solution without disruption of any aggregates prior to their on-line analysis with RI-MALS (Håkansson, Ulmius, & Nilsson, 2012; Ulmius et al., 2012). The amount, size and conformation of aggregates in dilute solution can be highly variable depending on a host of factors such as beta-glucan concentration, grain source, sample preparation, and sample solution and thermal history (Korompokis, Nilsson, & Zielke, 2018; Vårum et al., 1992).

In contrast, methods such as viscometry and SEC (e.g. see (Christensen et al., 2001), sedimentation velocity analytical ultracentrifugation (SV-AUC) (Channell et al., 2018; Woodward, Phillips, & Fincher, 1983) and osmometry (Channell et al., 2018; Vårum & Smidsrød, 1988; Vårum et al., 1992; Woodward et al., 1983) appear to mostly detect molecularly dissolved BG where any undissolved material has been removed by filtration or centrifugation prior to measurement. Shear forces in SEC columns and viscosity capillaries are thought to largely break-up and prevent the formation of beta-glucan aggregates. High centrifugal forces, typically employed in sedimentation velocity experiments, are hypothesised to remove any supramolecular aggregates of BG from optical registration, while membrane osmometry is deemed not sensitive enough to detect small fractions of very large beta-glucan aggregates (Vårum et al., 1992). Certain solvents may also be used to disrupt beta-glucan aggregation such as those typically used to dissolve cellulose (e.g., the copper amine complex Cuoxam $[Cu(NH_3)_4(H_2O)_2](OH)_2$ (Grimm et al., 1995). A solution of 0.5 M NaOH has been shown to prevent aggregation by electrostatic repulsion when studied by batch and dynamic light scattering (Li et al., 2011) but not when used as the solvent and carrier, in analysis by AF4-MALS-RI (Håkansson et al., 2012; Ulmius et al., 2012).

In this study we compare a variety of different methods to determine the weight-average molecular weight and molecular weight distribution of six isolates of BG. Three of these isolates are pure BG while the other three contain up to 20% of other impurities such as proteins. In six different laboratories we compare capillary viscometry, aqueous SEC-MALS-RI with on-line viscometry (VISC), SEC-FL, SEC-MALS-RI using *N,N*-dimethyl acetamide (DMAc)/0.9% lithium chloride (LiCl) as mobile phase, two different AF4-MALS-RI instruments, and SV-AUC. An additional set of sedimentation equilibrium experiments were performed on one of the samples (see supplementary data). Apart from DMAc/LiCl-SEC-MALS-RI, all the isolates were distributed to the participants in solution to eliminate inter-laboratory differences in dissolution and in this way make a true comparison of the methods. Furthermore, the stability of these BG in solution during 4 years of refrigerated storage in the dark was investigated using SEC-MALS-RI with the strategic aim of producing a wide range of molar mass standards using one common dissolution method.

2. Materials and methods

2.1. Materials

A purified oat beta-glucan isolate known as Oatwell 90 (BG 90, batch 12-GC, labelled in this study as RT-8) and beta-glucan enriched oat bran flour Oatwell 32 batch 1213 were a kind gift from Frederic Proton at Swedish Oat Fiber, Bua, Sweden. Isolates of BG from barley (High viscosity: Lot 90501b, RT-11) and oat (High viscosity: Lot 90802a, RT-12) were purchased from Megazyme, Bray, Ireland. Another purified oat BG isolate was a kind gift from Susan Tosh formally Agriculture and Agri

Food, Guelph, Canada and labelled RT-10. A barley flour enriched with bran containing 30% beta-glucan concentrate (Cerabeta™ lot 16133) was a free sample from Steve Jackway, GrainFrac Inc, Edmonton, Canada. All other chemicals were purchased from Merck KGaA, Darmstadt, Germany or affiliates.

2.2. Extraction and purification of beta-glucan from Cerabeta and Oatwell 32

The extraction and purification procedure used for BG is described in detail in Rieder et al. (2015). The only difference in the current study was that the pancreatin and xylanase treatments were omitted, and final drying of extracted BG involved washing in 96% ethanol and then oven drying at 60 °C. The Oatwell 32 derived isolate was labelled RT-7 while the Cerabeta derived isolate was labelled as RT-9.

2.3. Compositional analysis

The enzymic assay of AOAC method 995.16 from Megazyme was used to determine the content of BG in the freeze-dried isolates as weight percent of dry weight. Protein content was estimated by elemental analysis of total nitrogen multiplied by a factor of 6.25 using a Vario Cube elemental analyser. Ash (total mineral) content was analysed by gravimetric determination following combustion at 550 °C in a muffle furnace. Total starch content was measured by enzymic assay (AOAC 996.11). Arabinoxylan content was estimated by determination of arabinose and xylose following acid hydrolysis and their determination as corresponding alditol acetates by GC-FID (Englyst, Quigley, & Hudson, 1994). Fat content was determined gravimetrically after extraction into methanol/chloroform (Folch, Lees, & Stanley, 1957).

2.4. Preparation of beta-glucan standards in dilute aqueous solution

In April 2017 duplicate portions of 225 mg of each isolate of BG were weighed into 250 mL Duran glass bottles and then 4.5 mL of 80% aqueous ethanol was added and occasionally shaken over 1 h. A solution of 150 mL MilliQ water (18 MΩ) containing 0.02% sodium azide was then added to each of the sample bottles, which were placed in a bath of boiling water for 1 h and occasionally shaken. The bottles were then placed on their sides in an Innova 40R incubator shaker (New Brunswick Scientific) for 1 h at 70 °C operating at 400 rpm. Following a visual check, all samples apart from the BG extracted from Oatwell 32 and CeraBeta (RT-7 and 9, respectively) were dissolved. The RT-7 and -9 were further incubated for another hour. All samples were then subjected to centrifugation at 1750*g* at 20 °C in an Heraeus Multifuge 4 KR (DJB Labcare Ltd., Newport Pagnell, UK) centrifuge. All samples were then placed in a sterile laminar flow cabinet to avoid contamination with air borne beta-glucanases such as from wheat flour. These were then filtered through Millipore 0.8 μm syringe driven filters into 50 mL plastic centrifuge tubes, capped and placed into a boiling water bath for 10 min. The samples were then left to cool before they were stored in the dark at 4 °C until analysis, except for the time required for the shipment period (1–3 days) to send samples to the different laboratories for molar mass determination. Beta-glucan concentration was determined as above using AOAC method 995.26 (after filtration). Prior to analysis all laboratories were instructed to place the capped tubes containing the samples in a boiling water bath for 5–10 min. The BG were then analysed directly without any further filtration.

2.5. Preparation of beta-glucan standards in DMAc/0.9% LiCl

Freeze-dried samples equivalent to RT-7, RT-9 and RT-10 were treated according to a standard protocol used for cellulose, which is based on solvent-exchange from water to ethanol into DMAc (Potthast et al., 2015). The samples stayed 12h in DMAc and were dissolved in DMAc/LiCl 9% and diluted with DMAc prior to injection. Dry samples equivalent to RT-8, RT- 11 and RT-12 were partly dissolved already in DMAc prior to injection. Therefore, they were put into DMAc/LiCl 0.9% after the solvent-exchange from water to ethanol. After 24h on the shaker, DMAc/LiCl 9% was added for another 24h. The samples were diluted accordingly prior to injection.

2.6. Aqueous size-exclusion chromatography with multi-angle light scattering, refractive index and viscosity detection (SEC-MALS-RI-VISC) (Lab 1)

A Shimadzu LC-20 HPLC system operating at room temperature delivered 0.1 M sodium nitrate/0.02% sodium azide at 0.5 mL/min to a guard-column (Tosoh PWXL) and then to two serially connected size-exclusion columns (TosohTSK-gel G6000 PWXL followed by G5000PWXL). The injection volume was 100 μL. The detection system comprised of a serially connected Dawn Helios +8 eight angle light scattering photometer ($\lambda_0 = 633$ nm) (MALS), a Viscostar II viscometer (VISC) and an Optilab T-Rex differential refractive Index (RI) detector (all Wyatt, California, USA). All detectors were calibrated regularly. Astra version 6 (Wyatt, USA) was used to collect and process raw data. A first order ($R_2 = 0.99$) 'Zimm fit' to Kc/R_θ vs. $\sin^2(\theta/2)$ was used to construct a Debye plot to extrapolate to zero angle to compute *M*. A plot of M vs. elution time was then fitted to a first-order exponential within the region where detector sensitivity is high (acceptable $R_2 = 0.99$) and then forward and back extrapolated to higher and lower mass regions where the signal intensity of MALS and the RI detector is respectively low. The refractive index increment (dn/dc in mL/g) was taken to be 0.146 (a commonly used value for polysaccharides in aqueous solution) and A_2 was set to zero.

2.7. Aqueous size-exclusion chromatography with post-column calcofluor addition and fluorescence detection (SEC-FL) (Lab 1)

The HPLC system consisted of two pumps (Dionex UltiMate 3000), an auto injector (Dionex UltiMate 3000), a pre-column (Tosoh PWXL), two serially connected SEC columns (Tosoh TSK-gel G6000 PWXL followed by G5000PWXL, maintained at 40 °C) and a fluorescence detector (Shimadzu RF-10A, Shimadzu Europa, Duisburg, Germany). The eluent (50 mM Na_2SO_4) was delivered at a flow rate of 0.5 mL/min. The injection volume was 50 μL. Calcofluor (Megazyme) solution (25 mg/L in 0.1 M tris(hydroxymethyl)aminomethane) was delivered post-column through a T-valve at a flow rate of 0.25 mL/min. Fluorescence detection of the formed Calcofluor/BG complexes occurred at $\lambda_{ex} = 415$ nm and $\lambda_{em} = 445$ nm. A calibration curve for *M* of the BG was constructed with in-house *M* standards of BG and standards purchased from Megazyme with peak *M* from 31600 to 2418000. A proprietary third-order polynomial regression (PSS poly 3) was fitted to the retention time plotted against the peak *M* using PSS WinGPC Unichrome software (PSS Polymer Standard Service, Mainz, Germany).

2.8. DMAc/LiCl size-exclusion chromatography with multi-angle light scattering and refractive index detection (DMAc/LiCl SEC-MALS-RI) (Lab 2)

SEC analysis of the samples was carried out with DMAc/LiCl (0.9%, w/v) as the eluent (filtered through a 0.2 μm filter). The SEC consisted of an autosampler (Hewlett Packard 1100 series), a Kontron pump, a Dawn DSP multiple-angle light scattering (MALS) detector with an argon ion laser ($\lambda_0 = 488$ nm) (Wyatt Technology Corporation) and a RI detector (Shodex RI-71). The LS detector included 18 scattering angles. Four serial GPC columns (Agilent PLgel 20 μm Mixed-ALS 300 mm × 7.5 mm), an injection volume of 100 μl and a flow rate of 1.00 mL/min were used. The molecular weight distribution, and M_w were calculated with a dn/dc value of 0.136 (Potthast et al., 2015), which was determined for cellulose in DMAc/LiCl (0.9%, w/v) at 25 °C and 488 nm. A first order 'Zimm fit' was used to construct a Debye plot to extrapolate to zero angle

to compute *M*.

2.9. Capillary viscometry (Lab 3)

The samples of BG were diluted 1:1 with 0.2 M NaCl followed by heating for 5 min in a boiling water batch. Once cooled, a 14 mL sample was pipetted into the Ubbelohde glass capillary held at 20 °C under constant stirring. Each sample was serially diluted stepwise with 0.1 M NaCl down to a factor of 5 using a Radiometer ABU91 autoburette attached to an AVS control unit. Inputted concentrations were based on that measured for BG. Flow-through times were collected automatically. Relative (η_r) and specific (η_{sp}) viscosities were calculated and plotted according to Huggins (η_{sp}/c vs. c), Mead-Fouss ((ln η_r)/c vs. c), Billmayer ($2(\eta_{sp}-\ln\eta_r)]^{1/2}$/c), and Herman (log η_{sp}/c vs. c). Intrinsic viscosities [η] for each equation were obtained by linear regression with extrapolation to infinite dilution. Mean [η] was taken as $[\eta_w]$ of the BG. Weight (viscosity)-average molecular weight (M_w) was calculated by re-arranging the Mark-Houwink-Kuhn-Sakurada (MHKS) *M* -$[\eta]_w$ power law relation $[\eta_w] = KM^a$ to $M = ([\eta_w]/K)^{1/a}$. The scaling exponent (*a*) and constant (K) were obtained from double-logarithmic plots of *M* (g/mol x 10^3) against -$[\eta_w]$ (dl/g) from all the SEC-MALS-RI-VISC data (n = 11 for each sample) obtained by Lab 1 and fitted to a power function. The exponent *a* (slope) was 0.6 and y-intercept K was 0.178 dl/g.

2.10. Sedimentation velocity analytical ultracentrifugation (SV-AUC) (Lab 4)

Sedimentation velocity experiments were conducted in a Beckman (Palo Alto USA) XL-I AUC equipped with Rayleigh Interference optics. The 12 mm optical path length double sector cells with "Paley" phosphate-chloride buffer (pH6.8, I = 0.1M) were made up (Green, 1933) as the reference solvent and used in the reference channels. For each beta-glucan sample a low loading concentration of 0.33 mg/mL (after correction for radial dilution in the sector shaped ultracentrifuge cells) was chosen, with a rotor speed of 40,000 rpm and temperature of 20 °C. A differential sedimentation coefficient distribution g(*s*) of the sedimentation coefficient *s* was produced according to the SEDFIT algorithm (Dam & Schuck, 2004). The weight (sedimentation velocity)-average molecular weight was calculated by re-arranging the extended Fujita model power law relation $s_w = \kappa_s M^b$ to $M = (s_{w/}\kappa_s)^{1/b}$. The weight-average sedimentation coefficient s_w can be found from the sedimentation coefficient distribution through $\Sigma s_i c(s)_i/\Sigma c(s)_i$. A value of the sedimentation power law conformation parameter $b = 0.45$, previously found for cereal BG and consistent with a random coil conformation, was used (Channell et al., 2018). The intercept coefficient, κ_s was evaluated by rearranging the power law relation once more to $\kappa_s = (s/M^b)$ by taking the $s_{20,w}$ (*s* standardised to the density and viscosity of water at 20.0 °C – see Channell et al., 2018) at 0.33 mg/mL and *M* determined from SEC-MALS-VISC in Lab 1. Differential molecular weight distributions were then generated using these *b* and κ_s values from the differential sedimentation coefficient distribution by $f(M) = g(s).(ds/dM)$ where $ds/dM = b.\kappa_s^{1/b}.s^{(b-1)/b}$.

As an internal consistency check, and to calculate the weight-average sedimentation coefficient, plots of reciprocal weight-average of sedimentation vs. average sedimenting concentration (in g/mL and corrected for radial dilution) were fitted to the Gralén relation $1/s = 1/s^o(1+k_sc)$ as their limiting slope (Gralén, 1944) using the Microsoft Excel solver least squares fitting routine. From this one obtains the infinite dilution (non-ideality free) sedimentation coefficient s^o and the concentration dependence or Gralen coefficient k_s (mL/g) - not to be confused with the power law intercept coefficient κ_s - which can be related to molecular shape.

2.11. Asymmetric flow field-flow fractionation-MALS-RI (Lab 5)

Experiments were carried out in aqueous 0.1 M $NaNO_3$ (Sigma–Aldrich, Germany) (Mäkelä et al., 2015). A Postnova Analytics AF2000 MT AF4 system (autosampler, degasser, 2 isocratic pumps, 1 syringe pump) was serially connected to a 7-angle Brookhaven MALS operating at a wavelength of $\lambda_0 = 660$ nm and a Postnova PN 3150 RI detector. One of the isocratic eluent pumps was connected to an inline degasser to deliver 0.1 M $NaNO_3$ as carrier flow. The AF4 channel (335 × 60 × 40 mm) comprised a bottom plate with ceramic frit, a spacer with a thickness of 350 μm, and a top plate with flow outputs. The accumulation wall membrane was made from regenerated cellulose with cut-off value 10000 g/mol. Samples of 50 μL of BG (RT7-12) were injected. During the focusing step, a 7 min injection time with injection flow of 0.2 mL/min and 1 mL/min cross flow was used for all the samples. The crossflow was started at 1 mL/min and exponentially decayed (exponent = 0.3) to 0.15 mL/min. The detector flow was isocratic at 0.5 mL/min. A slot flow of 0.5 mL/min was maintained from the syringe pump to remove excess solvent from the upper part of the channel. AF2000 control software was used to collect and process raw data. To reduce RI baseline instability a blank signal (pure solvent) was subtracted from the run signal. A first order Zimm plot was used to calculate M. A dn/dc value of 0.146 mL/g for BG in aqueous solution was used.

2.12. Asymmetric flow field-flow fractionation-MALS-RI (Lab 6)

A Wyatt Eclipse AF4 system with Agilent 1260 Infinity II Quaternary Pump, Agilent 1260 Infinity II autosampler, Shimadzu CTO-20AC column oven was serially connected to a Shimadzu SPD-20AV UV detector, a Wyatt Dawn Heleos II MALS detector and a Wyatt OptiLab T-rEX RI detector. The channel was a Wyatt short channel with a spacer creating a nominal channel thickness of 350 μm. The accumulation wall membrane was made from polyethersulphone with a cut-off of 10 KDa (Wyatt Technology Europe GmbH, Dernbach Germany). For AF4 measurements a carrier liquid with 10 mM $NaNO_3$ was used. For injection/focusing, 30 μL of beta-glucan samples (RT7-12) were injected at a flow rate of 0.2 mL/min for 1.5 min, followed by a 2.5 min focus step (focus flow 1.5 mL/min). The crossflow was started at 3 mL/min and exponentially decayed over 30 min to 0.05 mL/min. The detector flow was isocratic at 1.0 mL/min. The instrument was operated by the software Vision (2.0.2.9). Data collection and evaluation were controlled by Wyatt ASTRA (8.0.0.28). To reduce RI baseline instability a blank signal (pure solvent) was subtracted from the run signal. A first order 'Berry fit' was used (Nilsson, 2013) to construct a Debye plot for 12-angles to calculate *M*. The refractive index increment was taken to be 0.146 and A_2 was set to zero.

2.13. Analysis timetable and storage stability

All initial analysis were completed within 6 months of preparing the BG samples. The results for analytical ultracentrifugation were collected in the summer of 2020. Samples were repeatedly analysed in approximately annual intervals over 3.5 years using Lab 1 SEC-MALS-VISC-RI to assess storage stability.

3. Results

The six isolates of BG prepared for this study originated from oat and barley. Three of these (Oatwell 90, RT-8, and the two Megazyme samples RT-11 and 12) were found to contain almost exclusively BG at a purity >94% (Table 1). The polysaccharide extracted from a BG enriched barley fraction (RT-9) was also confirmed to have a high beta-glucan content (88% BG, 1.5% protein) while the two samples extracted from oat (RT-7 and RT-10) contained slightly less BG, 79 and 77% respectively, and between 5.0 and 9.5% protein (Table 1). Starch, fat, ash (total minerals) and arabinoxylan were only present in trace amounts (ca. <3%) (Table 1), apart from fractions RT-9 and RT-10 which were estimated to contain between 4 and 6% arabinoxylan.

Table 1
Source, gross composition (mean n = 2, g/100 dry weight ± SD) of beta-glucan extracts RT-7 – RT-12 and the dissolved concentration (mg/mL) of beta-glucan in samples distributed to Labs 1–6 conducting aqueous based analysis methods. [1]Due to lack of available sample n = 1.

Sample code	Source of beta-glucan extract	Beta-glucan	Protein	Starch	Arabinoxylan	Fat[1]	Ash[1]	Total	Beta-glucan concentration in solution
RT-7	Oatwell 32	79 ± 2.4	9.4 ± 0.05	0.3 ± 0.01	2.0 ± 0.02	0.9	1.7	93.3	1.03 ± 0.03
RT-8	Oatwell 90	95 ± 1.9	0 ± 0	0.2 ± 0.01	0.9 ± 0.01	0.3	3.1	99.5	1.2 ± 0.02
RT-9	Cerabeta barley	88 ± 3.1	1.5 ± 0.08	0.2 ± 0.04	4.3 ± 0.02	1.45	0.9	96.4	1.15 ± 0.04
RT-10	Agri-Food Canada oat	77 ± 2.8	5.1 ± 0.05	2.6 ± 0.02	6.0 ± 0.01	0.7	1.6	93,0	1.02 ± 0.04
RT-11	Megazyme barley	96 ± 1.8	0 ± 0	0.1 ± 0	0.2 ± 0.02	0.3	0.1	96.7	1.24 ± 0.02
RT-12	Megazyme oat	94 ± 0	0 ± 0	0.1 ± 0.02	0.6 ± 0.01	2.9	0.7	98.3	1.21 ± 0

Moisture contents ranged typically between 5 and 10%. The concentration of BG in the aqueous samples distributed to the different laboratories were between 1.02 and 1.24 mg/mL (Table 1).

Fig. 1A–C shows the elution curves for intensity of scattered light, refractive index and specific viscosity for RT7-12 obtained by Lab 1 using aqueous SEC-MALS-VISC-RI. All traces are unimodal with an absence of any shoulders. The area under the curve of the refractive index signal is similar for all samples (concentration dependent) while for the light scattering and viscosity signals, a size dependence of signal response is observed. These observations indicate consistent recovery. Samples RT 7 and 9 start to elute at almost the same time with the ascending part of the peak overlapping indicating these molecules are part of the excluded column volume.

In Fig. 1D showing a semi-log plot of calculated *M* versus elution volume, for the elution interval with both a good RI and light scattering intensity, the samples containing almost exclusively BG (RT-8, RT-11 and RT-12) overlap one another and fit to a common first-order exponential function. In contrast, both RT-7, and RT-9, which contain slightly less BG (79 and 88%, respectively, Table 1) and were produced by the same method with thermostable alpha-amylase treatment, clearly fit to a different first-order exponential with higher masses eluting at corresponding elution volumes (Fig. 1D). Sample RT-10, with the lowest purity of BG (77%), lies in a similar region to RT-8, RT-11 and RT-12 at lower elution volumes but clearly departs at higher elution volumes and therefore has a different linear fit.

Examination of double logarithmic plots of molar mass versus

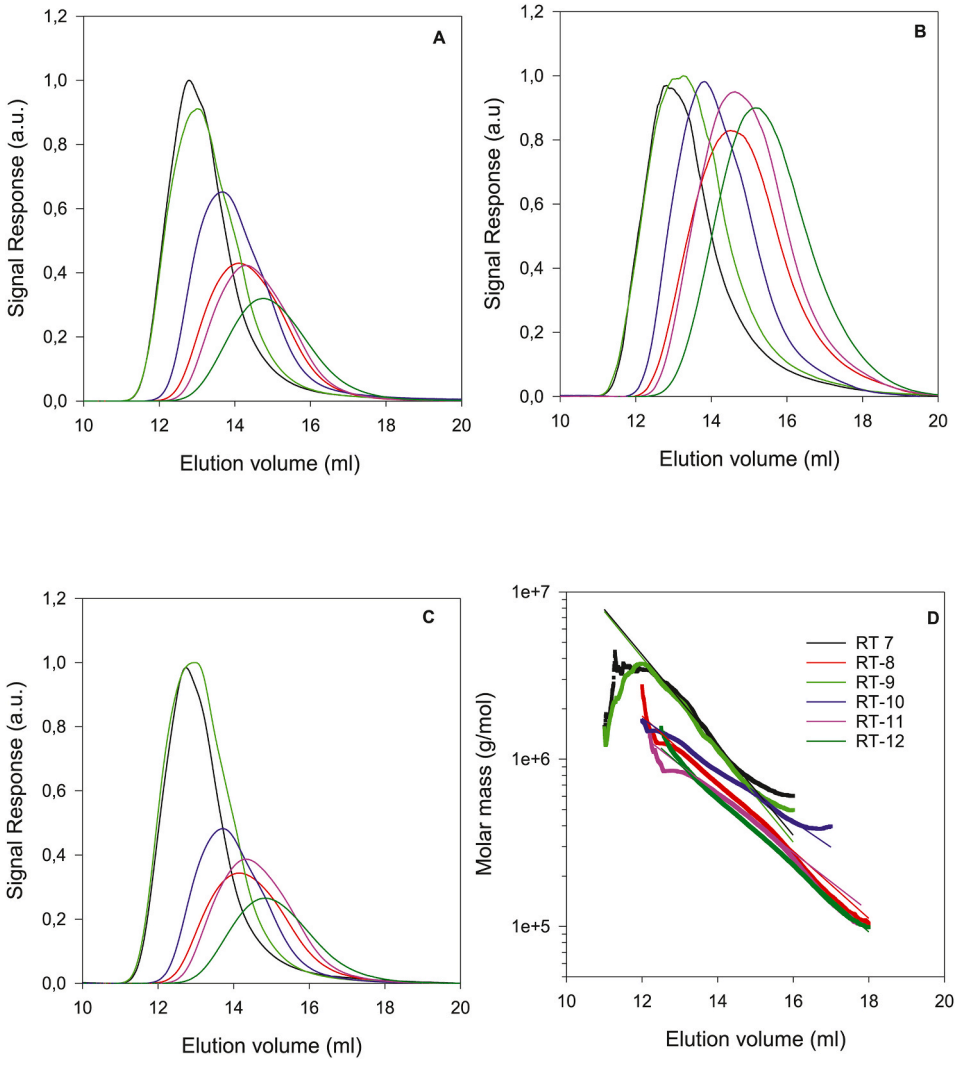

Fig. 1. Chromatograms (A–C) of beta-glucan samples RT-7 - RT-12 obtained by SEC-MALS-VISC-RI (Lab 1). (A) The intensity of scattered light (Rayleigh ratio) from MALS, (B) Refractive Index (RI), (C) Specific viscosity, (D) Calculated molar mass versus elution volume with a corresponding first-order exponential fit.

Table 2
(**A**) Calculated weight-average molar mass (x10^3 g/mol) beta-glucan determined by a range of different methods. SD = standard deviation; numbers in superscript for SD values indicate number of replicates. (**B**) Minimum (Min) and Maximum (Max) determined weight-average molar mass (x10^3 g/mol) of BG. [1]Repeated measurements between April – September 2017.

A

Method	Aqueous-SEC-MALS-VISC-RI[1]		DMAc/LiCl SEC-MALS-RI			SEC-Calcofluor-FD			Capillary Viscometry			SV		AF4-MALS-RI (Lab 5)		AF4-MALS-RI (Lab 6)		
Sample		SD[11]			SD[2]			SD[2]			SD[2]		SD			SD[2]		SD[3]
RT-7	2103	151	1747		18.5	1160		3	1636		17	2100	–	1785		49	6866	95
RT-8	547	28	668		6.4	596		1	499		20	500	–	646		152	1011	24
RT-9	1822	110	1744		22.5	1130		4.5	1441		304	1800	–	2335		219	8079	453
RT-10	879	35	1057		54.4	848		3.5	721		206	880	–	1030		28	13241	482
RT-11	468	14	603		23.3	558		0.5	472		53	470	–	441		58	892	22
RT-12	343	10	471		13.4	410		4.5	353		70	330	–	558		299	1139	79

B

Method	Aqueous-SEC-MALS-VISC-RI1		DMAc/LiCl SEC-MALS-RI			SEC-Calcofluor-FD			Capillary Viscometry			AF4-MALS-RI (Lab 5)			AF4-MALS-RI (Lab 6)	
Sample	Min		Max	Min		Max	Min		Max	Min		Max	Min		Max	Min	Max
RT-7	1844		2316	1728		1765	1157		1162	1619		1653	1750		1820	6759	6941
RT-8	500		598	663		672	595		597	479		520	539		754	995	1039
RT-9	1627		1957	1722		1767	1125		1134	1137		1745	2180		2490	7755	8596
RT-10	829		925	1018		1095	844		851	514		928	1010		1050	12777	13740
RT-11	444		489	586		619	557		558	419		524	400		482	866	905
RT-12	324		355	461		480	405		414	283		422	346		769	1083	1229

Fig. 2. Weight-average molar mass for beta-glucan samples RT-7 - RT-12 (mean ± SD) determined by aqueous SEC-MALS-VISC-RI as a function of storage time between 2017 and 2020 (Lab 1). SD = standard deviation.

intrinsic viscosity (MHKS)-plot (data not shown) mirrored trends seen in Fig. 1D. The scaling coefficients *a* (slope) of fitted power law equations (mean, n = 11, ±SD) were between 0.58 ± 0.01 – 0.6 ± 0.03 for the pure BG (RT-8, RT-11 and RT-12) yet slightly lower for the RT-10 sample at 0.54 ± 0.06, and even lower for RT-7 and RT-9 (0.50 ± 0.08).

Another way to visualise MHKS data is to make a log-log plot of the weight-average intrinsic viscosity ($[\eta]_w$) and M_w values obtained from SEC-MALS-VISC-RI (using a first-order fit extrapolation to lower and higher elution volumes). Evaluation of such a plot using all samples (RT-7-12) together yielded a scaling coefficient a of 0.6 while the y intercept k was 0.178 dl/g ($R_2 = 0.94$).

SEC-MALS-VISC-RI analysis of all samples (RT-7-12) revealed a mean M_w of between 343–2103 × 10^3 g/mol (Table 2). From 11 sets of analysis spanning a 5-month period, the standard deviations for determined replicate M_w's were small and between 10–35 × 10^3 g/mol - except for samples RT-7 and RT-9. For these two samples, standard deviations were 151 and 110 × 10^3 g/mol, respectively (Table 2A). For RT-7 and RT-9 the minimum measured values were 1844 and 1627 while the maximum values were 2316 and 1957 × 10^3 g/mol, respectively (Table 2B).

All the solutions of BG analysed by SEC-MALS (Lab 1) showed a polydispersity (M_w/M_n) of between 1.2 and 1.4. Repeated analysis of the same samples by SEC-MALS-VISC-RI after approximately 1-year intervals of storage at 4 °C over a four-year period revealed the samples in solution to be highly stable with no changes greater than ±10% in determined M_w (Fig. 2). This suggests an absence of storage-induced irreversible aggregation phenomena or chain-scission.

Weight-average intrinsic viscosities $[\eta]_w$ obtained by Lab 3 using SEC-MALS-VISC-RI are shown in Table 3. They range from 574 mL/g for RT-12 up to 1734 mL/g for RT-7. Fig. 3 displays Huggins, Mead-Fouss and Billmayer plots obtained from analysis of RT-7-12 by Lab 2 using capillary viscometry. All models fit the raw data to linear regression lines very well and the calculated $[\eta]_w$ values obtained by extrapolation to infinite dilution are very similar for all samples. The mean $[\eta]_w$ values from capillary viscometry are shown in Table 3. Excellent agreement was found between the values obtained by SEC-viscometry (Lab 1) and those obtained by $[\eta]_w$ capillary viscometry, as indicated by the $[\eta]_w$ SEC-viscometry ratios between 0.96 and 1.24 (Table 3).

Using the MHKS values for the scaling exponent (*a*) and the intercept parameter (K), obtained from plotting the M_w and $[\eta]_w$ for all samples on one double logarithmic plot (Lab 1), allowed calculation of an estimate for M_w from $[\eta]_w$ values obtained from capillary viscosity. In Table 2A and B, a comparison of the calculated M_w between the two methods showed a good agreement in calculated means, especially for the

Table 3
Weight-average intrinsic viscosity (mL/g) determined by aqueous-SEC-MALS-VISC-RI (Lab 1) compared with weight-average intrinsic viscosity determined by capillary viscometry at Lab 3 (mL/g) of beta-glucan samples. [1]Repeated measurements between April–September 2017, n = 11. [2]Duplicate runs. SD = standard deviation.

	SEC-viscometry[1]		Capillary Viscometry[2]		$[\eta]_w$ capillary/$[\eta]_w$ SEC
Sample					
		SD		SD	
RT-7	1701	151	1512	7	1.13
RT-8	770	28	742	13	1.04
RT-9	1734	110	1394	126	1.24
RT-10	997	35	916	113	1.09
RT-11	779	14	716	34	1.09
RT-12	574	10	600	51	0.96

samples containing the most BG (RT-8, RT-11 and RT-12), but for RT-7 and RT-9 a difference of up to 500 × 10^3 g/mol was found. Generally though, replicate capillary viscosity measurements had a higher variability than SEC-MALS-VISV-RI (Table 2B). Although values for the scaling coefficient *a* were accurately obtained from SEC-MALS-VISC-RI plots of *M* versus [η], the estimated values for the intercept parameter k proved much more variable and were therefore deemed unusable for conversions of capillary viscometry $[\eta]_w$ to corresponding M_w's.

Fig. 4A shows a plot of the sedimentation coefficient distribution g(*s*) vs. *S* at the lowest sedimentation concentration (corrected for radial dilution) of 0.33 mg/mL. Two types of distribution were observed. The samples comprising >94% BG (RT-8, RT-11 and 12) displayed a unimodal single peak Gaussian type distribution. On the other hand, the single peaks in samples RT-7, RT-9 and RT-10 showed a tendency for tailing at lower sedimentation coefficients. While all samples had a peak apex between 3 and 5S the overall distribution ranged from between 1

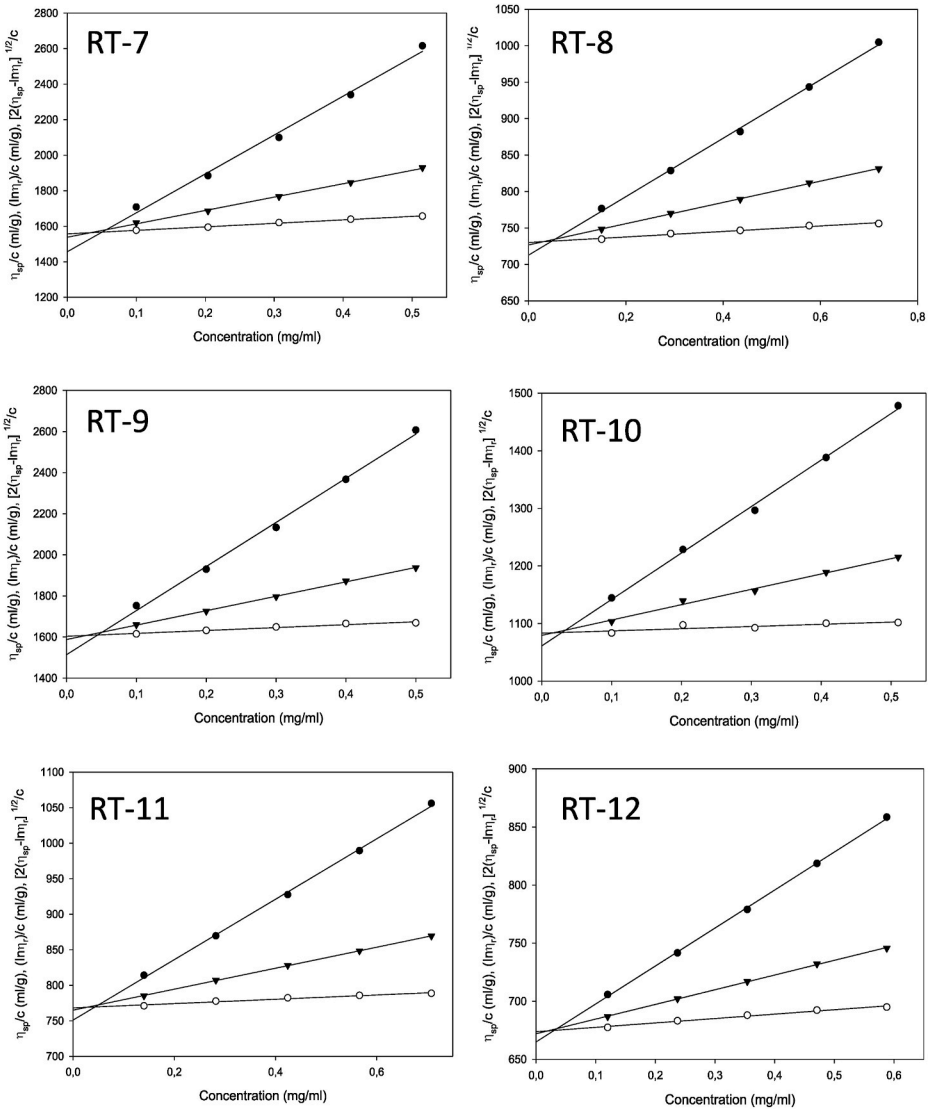

Fig. 3. Huggins, Mead-Fouss and Billmayer plots for beta-glucan samples RT-7 - RT-12 obtained by capillary viscometry (Lab 3).

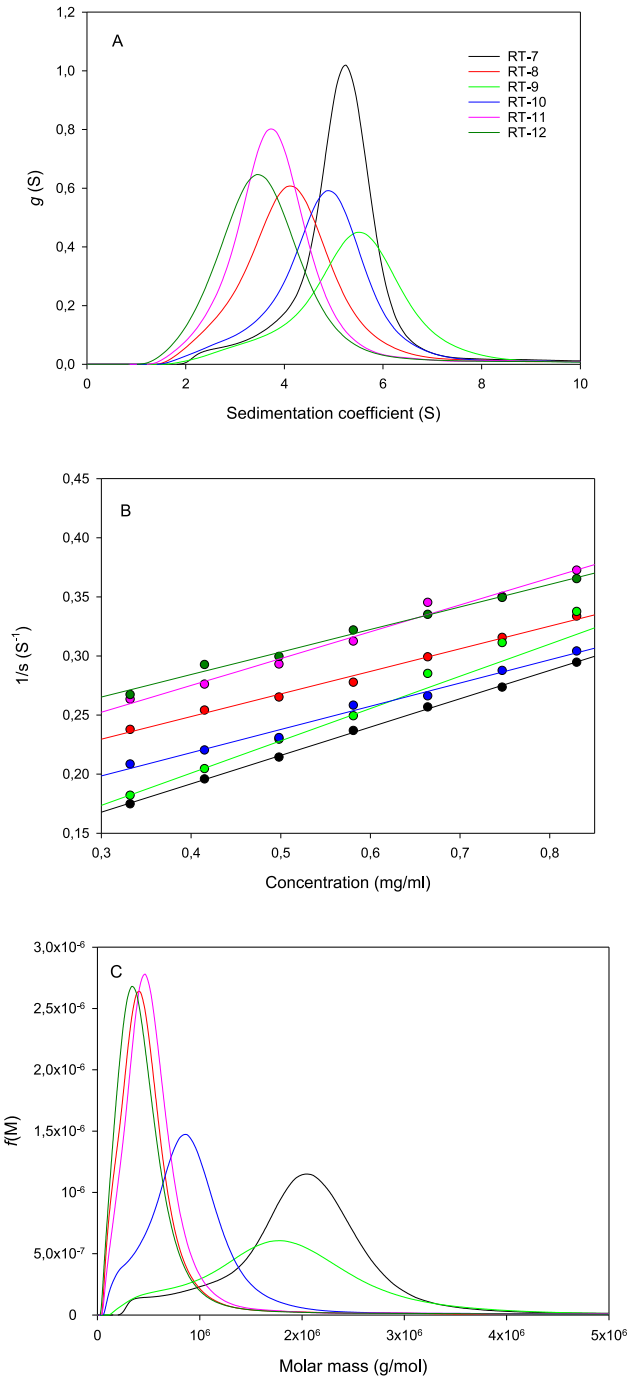

Fig. 4. Differential sedimentation coefficient distributions (A), Concentration dependencies of the (reciprocal) sedimentation coefficients (B), and Differential molar mass distributions (C) for beta-glucan samples RT-7 - RT-12 obtained from sedimentation velocity analytical ultracentrifugation (Lab 4).

and 9 S (Fig. 4A). In agreement with results and trends observed from SEC-MALS-VISC-RI, and capillary viscometry, samples RT-7, RT-9 and RT-10 have the largest average sedimentation coefficients (extrapolated to infinite dilution) of 7.2–13.7 S (Table 4) while for RT-8 and RT 11–12 lower s^0 values of 4.8–5.8 S were observed (Table 4).

As expected, a near linear increase in average reciprocal sedimentation coefficient was seen for each sample as a function of an increasing average sedimentation concentration (Fig. 4B). The exception was for RT-9 where only the limiting slope was fitted (Fig. 4B). The concentration dependence of sedimentation (Gralén coefficient) obtained from plots of $1/s$ vs. c ranged from 2979 mL/g for RT-9 down to 917 mL/g for

Table 4
The infinite dilution sedimentation coefficient (s^o in Svedbergs, S), Gralen coefficient (k_s in mL/g) and Wales van Holde ratio $k_s/[\eta]$ of beta-glucan samples determined by sedimentation velocity analytical centrifugation. Intrinsic viscosity values are taken from aqueous-SEC-MALS-VISC-RI measurements (data shown in Table 3).

Sample	s^0	k_s	$k_s/[\eta]$
RT-7	10.40	2500	1.5
RT-8	5.80	1110	1.4
RT-9	13.70	3000	1.7
RT-10	7.20	1410	1.4
RT-11	5.40	1235	1.6
RT-12	4.80	917	1.6

RT-12 (Table 4). Combining this data with SEC-derived [η] gives the hydration independent shape factor known as the Wales-Van Holde ratio with values ranging between 1.4 and 1.7 (Table 4), corresponding to a random coil conformation (close to Burgers theoretical value of 1.66) (Wales & Van Holde, 1954). Furthermore, an MHKS power law plot of sedimentation coefficient vs. M_w from SEC-MALS-VISC-RI had a slope of 0.46 (Supplementary Fig. 1) corresponding to a random coil conformation. This confirmed the use of the power law coefficient $b = 0.45$ obtained earlier (Channell et al., 2018) in the Extended Fujita method (Harding et al., 2011) for transforming the g(s) vs. s plots into molecular weight distribution plots $f(M)$ vs. M.

Transformation of the g(s) vs. S plot (Fig. 4A) to the differential weight - molar mass distribution (MMD) (Fig. 4C) again gave two distinct types of distribution. For the pure RT-8, RT-11 and RT-12 BG samples, a Gaussian-type unimodal distribution was observed albeit with minor tailing towards higher molar masses (Fig. 4C). In contrast, for the rest of the samples, barring RT-8, there was a tendency for a bimodal distribution manifest as a shoulder to the main peak (Fig. 4C). This points to the possibility of two populations of molecules, one dominated by BG and another possibly containing impurities. The peak apex corresponded well with calculated M_w values (Table 2) and, not surprisingly, matched consistently with the M_w values obtained from aqueous-SEC-MALS-VISC-RI (Table 2). Moreover, the capillary viscosity measurements were in almost perfect agreement with values from Lab 1 analysis using SEC-MALS-RI-VISC. This is explained, however, by the fact that MHKS scaling coefficients from the latter were used as a basis to determine M_w (via power law relations) from the sedimentation and capillary viscosity data.

Finally, and as a check for consistency, sedimentation equilibrium was performed on one of the samples (RT-8) at loading concentrations of 0.7 and 0.8 mg/mL. Because of the broadness of the distributions shown by Fig. 4A and C, several equilibrium speeds were recorded. In this case, the apparent weight-average molar masses increased at reduced rotor speed (Supplementary Fig. 2), attributed to less of the M distribution being lost from optical registration at the cell base. The lower rotor speeds and lower hydrostatic pressure may also lead to less disruption of any aggregates if present. A linear extrapolation yields for $M_{w,app}$ ~510 ± 30 kDa at 0.7 mg/mL and 480 ± 40 kDa at 0.8 mg/mL. Making an allowance for non-ideality using literature data (Harding, 1992; Woodward et al., 1983), a value for M_w ~600 kDa was obtained within reasonable agreement of the SEC-MALS-VISC result reported by Lab 1.

Elution curves for intensity of scattered light and refractive index for DMAc/LiCl SEC-MALS-RI (Lab 2) are shown in Fig. 5A and B. Although they look identical the curves in each plot are in fact different. As seen in the chromatograms obtained with aqueous SEC-MALS-VISC-RI (Lab 1, Fig. 1A and B), the form of the elution curves is similar albeit with a slightly larger tendency for tailing. In contrast, however, the area under the elution curves for the RI signal differ (Fig. 5B). Smaller areas are evident for the less DMAc-soluble and less pure BG samples of generally larger M (RT-7, RT-9 and RT-10) compared to the larger areas observed for the samples containing >94% BG of generally lower M (RT8 and 11), but not for sample RT-12, which also had a smaller area under the curve

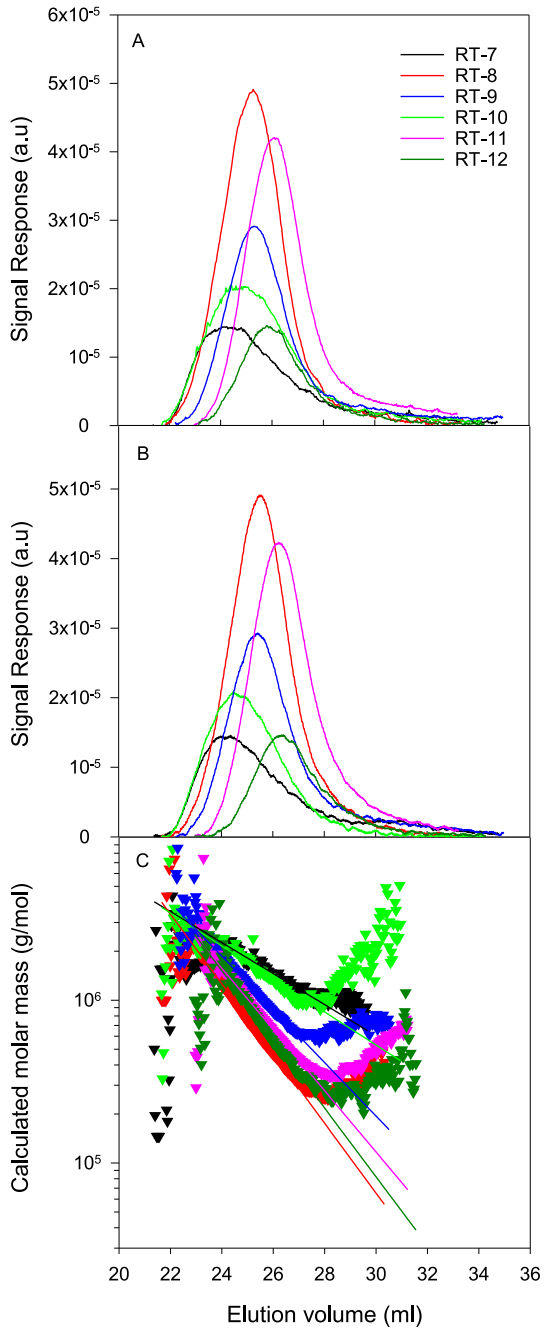

Fig. 5. Chromatograms (A and B) of beta-glucan samples RT-7 - RT-12 obtained by DMAc/LiCl SEC-MALS-RI (Lab 2). (A) The intensity of scattered light (Rayleigh ratio) from MALS, (B) Refractive Index (RI), and (C) Calculated molar mass vs. elution volume with a corresponding linear fit.

(Fig. 5B). The semi-log plot of calculated molar mass versus elution volume (Fig. 5C) is also similar to that observed for the aqueous SEC-MALS-VISC-RI method used in Lab 1 (Fig. 1D). The curves for samples containing >94% BG (RT-8, RT-11 and RT-12) are close to one another and fit to a similar first-order exponential function. Samples RT-7 and RT-9, likewise, both fit to a different first-order exponential function with again sample RT-10 showing an intermediate response. These observations support the contention that there are differences in polymer conformation as an apparent function of BG content and/or BG M_w.

Fig. 6A and Table 2A show the differential weight MMD and M_w values (F_w (log M) d(log M)), respectively, obtained from DMAc/LiCl SEC-MALS-RI. These can be compared with both aqueous-SEC-MALS

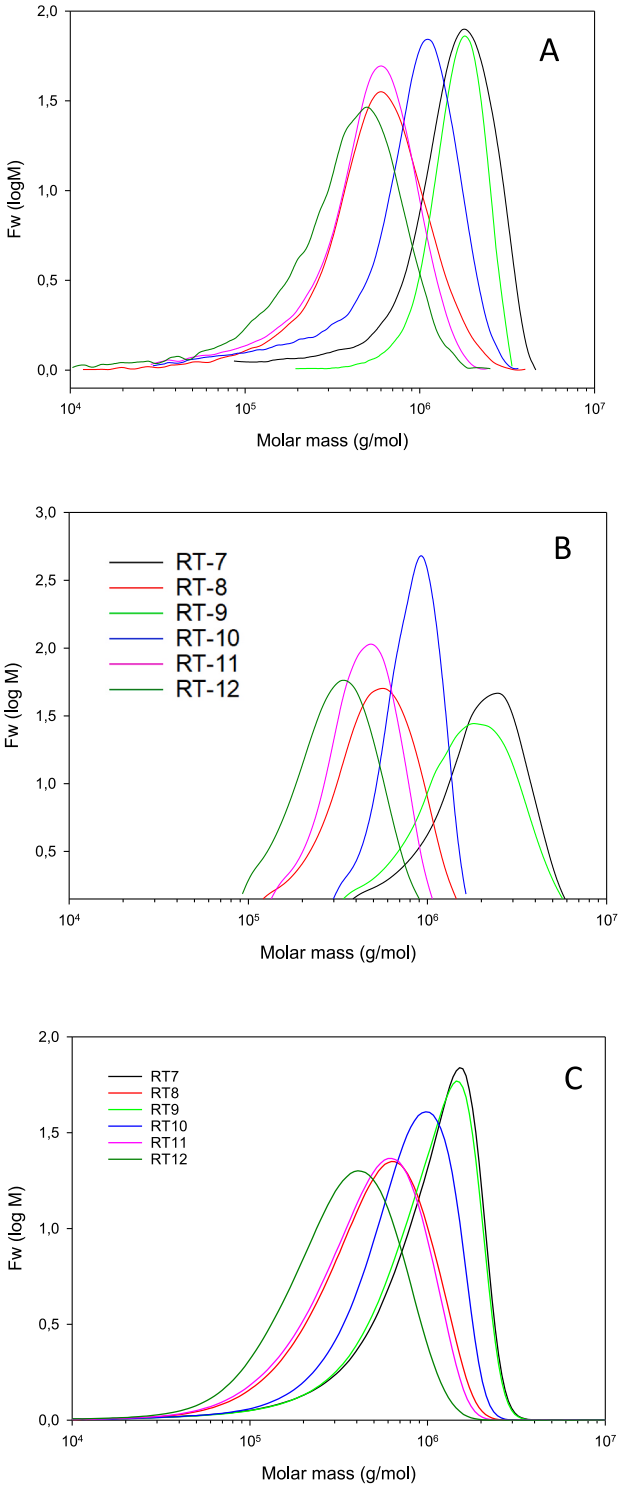

Fig. 6. Differential weight molar mass distribution of BG RT-7 - RT-12 obtained by (A) DMAc/LiCl SEC-MALS-RI (Lab 2), (B) SEC-MALS-VISC-RI (Lab 1) and (C) SEC-FL (Lab 1).

differential weight MMDs (Fig. 6B) and those derived from SEC -FL (Fig. 6C). The first observation is that all the samples displayed a general unimodal Gaussian-like distribution (Fig. 6). However, the MMD's obtained from SEC-calcofluor-FL (Fig. 6C), and to a lesser extent DMAc/LiCl SEC-MALS-RI (Fig. 6A), were found to be truncated towards higher M's $> 10^6$ g/mol. Interestingly, for both these methods samples RT-7

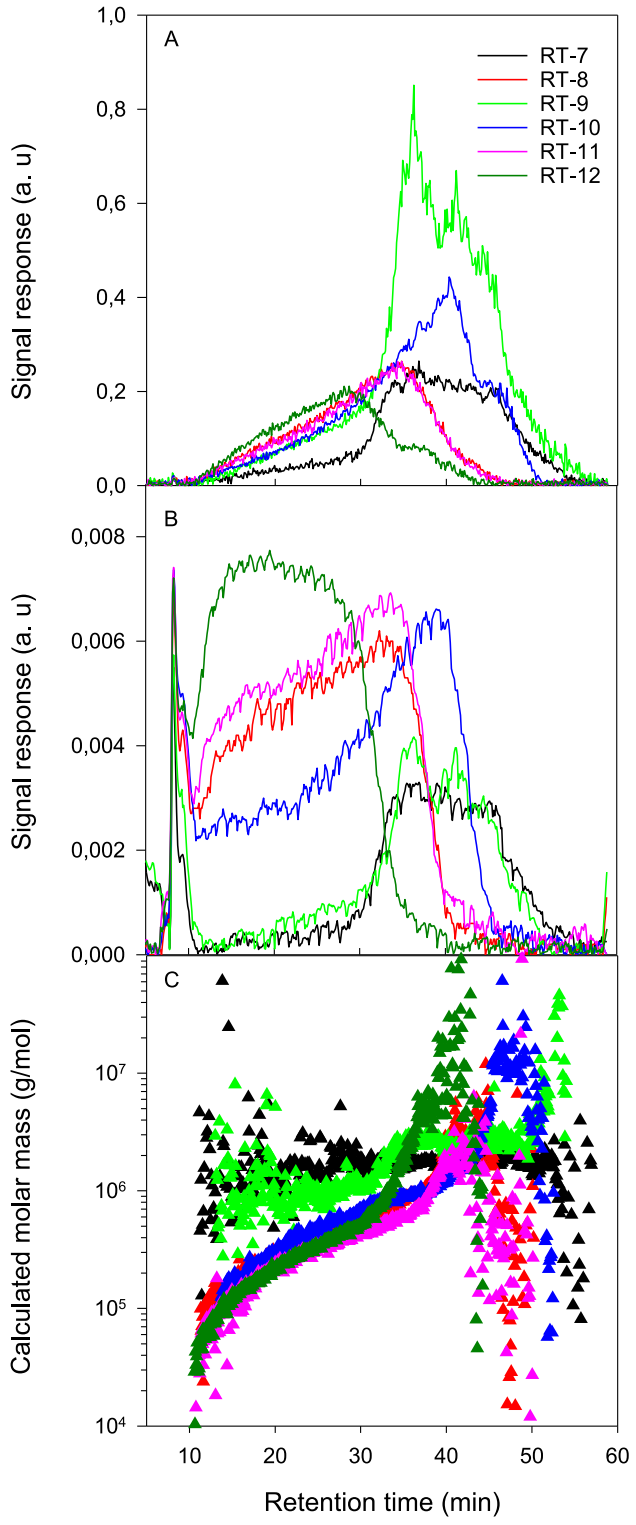

Fig. 7. Fractograms (A and B) of beta-glucan samples RT-7 - RT-12 obtained from AF4-MALS-RI (Lab 5). (A) The intensity of scattered light (Rayleigh ratio) from MALS, (B) Refractive Index (RI) and (C) Calculated molar mass vs. elution volume.

and RT-9 displayed an almost identical MMD as did samples RT-8 and RT-11 (Fig. 6C). Comparable *M*'s to SEC-light scattering were obtained for samples with the smallest *M*, and highest BG content (RT-8 and RT10-12). Yet for samples with a much larger *M* (RT-7 and RT-9) and lower BG content, lower overall *M* 's were determined (Table 2A) by SEC-FL with a maximum at 1100 $\times$ 10^3 g/mol, compared with the other samples. DMAc/LiCl SEC-MALS-RI, on the other hand, returned slightly higher calculated M_w values (500–700 $\times$ 10^3 g/mol) for RT-8, RT-11 and RT-12 and slightly lower values than aqueous SEC-MALS-VISC-RI for RT-7, RT-9 and RT-10 (Table 2). Duplicate measurements with both DMAc/LiCl SEC-MALS-RI and SEC-FL, respectively, were almost identical (Table 2B).

Two different AF4-MALS-RI systems were also evaluated (see methods for details). The fractograms in Fig. 7A and B shows the Rayleigh ratio and RI signals obtained with the system used at Lab 5. These fractograms, especially the RI signal, are a little noisy. They still display generally one peak, but they are broader, have a flatter apex and have a large shoulder at lower retention times compared to those observed with SEC-based methods (Fig. 1A and B). In AF4, the smallest molecules, which have the largest diffusion coefficients, are retained the least. At the start (5–10 min) of the RI fractogram there is a large peak (Fig. 7B). However, this peak has basically no light scattering signal due to the small size of these molecules, and they therefore contribute negligibly to *M*. The semi-log plot of calculated *M* versus retention time (Fig. 7C) are similar for all samples RT-8 and RT-10-12. At least two distinct linear regions between *M*'s of 10^5–10^6 g/mol and *M*'s $>$ 10^6 are noted (Fig. 7C). There is a much more rapid increase in *M* indicating a possible change in conformation, which may involve a transition to molecular aggregates. However, when examining the fractogram of the corresponding RI signal, these aggregates represent a small proportion of the total sample (see Fig. 7B). Apart from this difference, the overall trends (albeit mirrored) are comparable to those seen for SEC-MALS-VISC-RI (Lab 1). The samples with highest BG content follow a common *M* versus retention time plot, while RT-7 and RT-9 (less pure BGs) clearly show a different plot with a much slower and almost flat increase of *M* as a function of retention time. As observed with SEC methods this points to a difference in their conformation compared to samples with the highest content of BG. An exception is the RT-10 sample, which this time follows more closely the data of other pure BG (Fig. 7C) in the *M* versus retention time plot. A slightly higher variability in the AF4 data relative to data from the SEC based methods between duplicate analysis was noted (Table 2B).

The fractograms obtained with the AF4 system used by Lab 6 displayed a sharper, less noisy, and more pronounced Gaussian type peak than that reported by Lab 5. The shoulders in the RI signal (Fig. 8B) at lower retention times were generally smaller. In the light scattering signal (Fig. 8A) there was an absence of shoulders. As for the SEC-MALS-VISC-RI method used at Lab 1, samples RT-7, RT-9 and RT-10 displayed the most intense light scattering signal (Fig. 8A), while the areas under the RI signal curve for each sample were almost identical as evidenced by similar calculated recovered masses. Based on the known amount of BG injected (Table 1), Lab 6 analysis showed that the percentage recovery values calculated from the integrated RI signal, starting at 12–16 min (Fig. 8B), were between 96 and 107% for all samples.

The semi-log plot of calculated *M* versus retention time (Fig. 8C) seems to show at least three distinct linear regions for most samples, while for RT-9 four distinct linear regions can be seen. Region I includes molecules with calculated masses ranging from around 5 $\times$ 10^4–5 x 10^5 g/mol and a retention time up to 20 min. While RT-7, RT-8, RT-11 and RT-12 generally overlap, RT-9 and RT-10 are separate. In linear region II, extending from masses of about 5 $\times$ 10^5 to 5 $\times$ 10^6, it is seen that RT-8 and RT-11 overlap one another. All the other BG samples follow a slightly steeper trajectory with the linear region extending up to masses of about 10^7. A third linear region (III) is then evident with a steep increase in *M* with retention time for all samples except RT-9. For this sample, the increase in *M* levels out between 22 and 27 min retention time before rapidly increasing in a fourth linear region (IV) in a similar way to the other samples albeit at longer retention times.

While the calculated M_w determined from the AF4 system used in Lab 5 were fairly similar (perhaps RT-7 and RT-9 are an exception) to

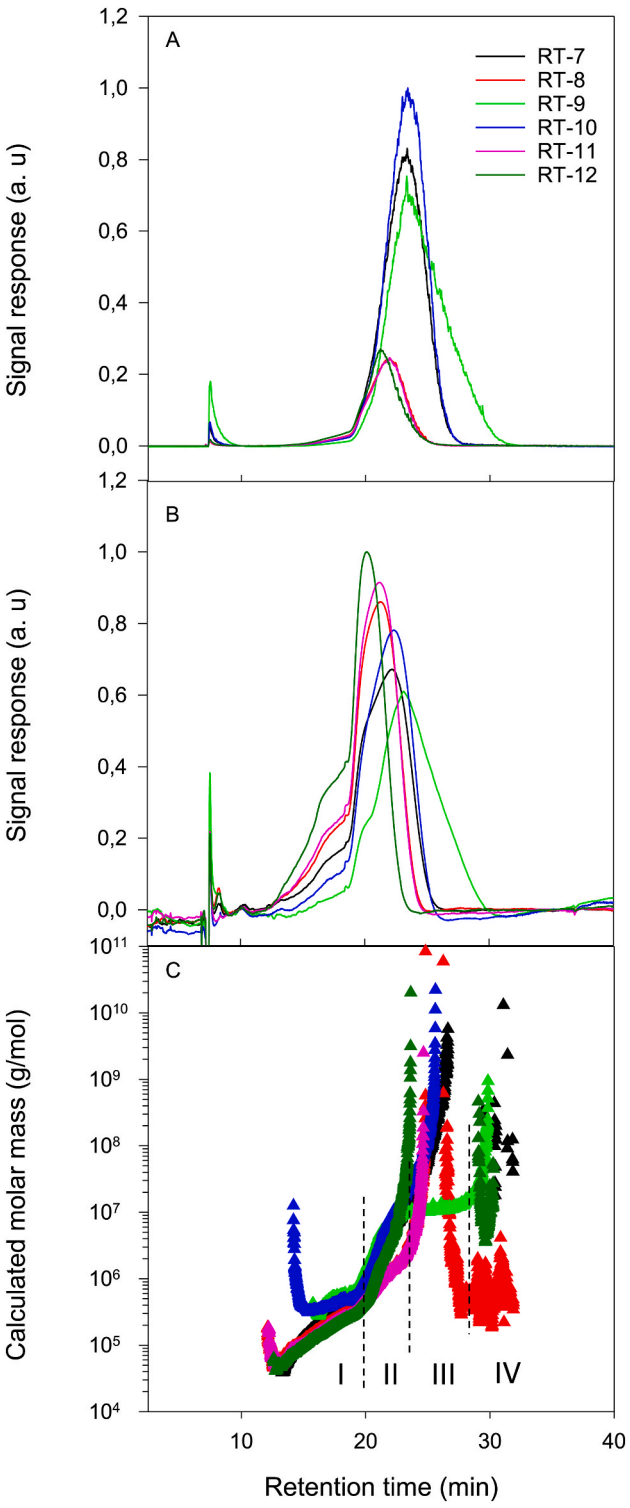

Fig. 8. Fractograms (A and B) of beta-glucan samples RT-7 - RT-12 obtained from AF4-MALS-RI (Lab 6). (A) The intensity of scattered light (Rayleigh ratio) from MALS, (B) Refractive Index (RI) and (C) Calculated molar mass vs. elution volume. Different distinct linear relations of *M* vs. retention time are marked by dashed lines and labelled regions I-IV.

samples determined by the SEC methods, capillary viscosity and SV (Table 2), the weight-average values from the AF4 analysis at Lab 6 were much higher both in terms of calculated M_w (Table 2) and span of the MMD (Fig. 9). For example, in the analysis of RT-7 in Lab 5 using AF4, the M_w was found to be 1760 $\times$ 10^3 g/mol, but using the same technique

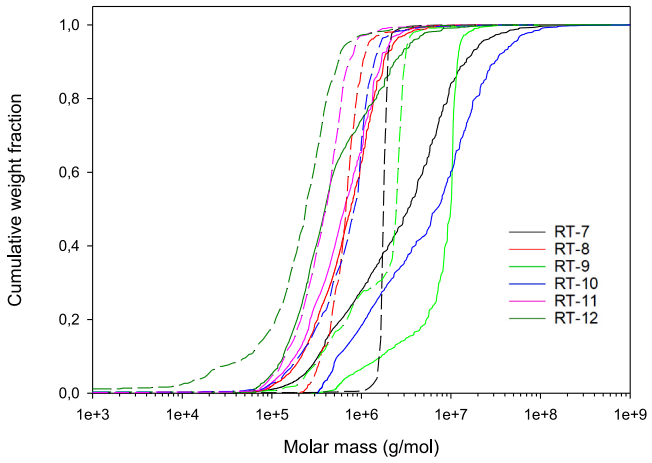

Fig. 9. Comparison of cumulative weight distribution of beta-glucan samples RT-7 – RT-12 from AF4-MALS determined by Lab 5 (dashed line) and Lab 6 (solid line).

in Lab 6, the *M* for this sample was over three times larger at 6866 $\times$ 10^3 g/mol. Similar trends were observed for all the other BG samples (Table 2). For sample RT-10, the calculated M_w reported by Lab 6 was over a decade higher at 13241 $\times$ 10^3 g/mol, than that observed in Lab 5. These differences between measurements at Labs 5 and 6 for each sample are nicely illustrated by the cumulative weight distribution plots (Fig. 9). In Lab 6, for the impure BG samples RT-7, RT-9 and RT-10 approximately 20–40% of the detected species had a molar mass >10^7 and a very large range of MMD. Interestingly, the RT-7 and RT-10 samples extracted from oat, followed a similar profile in the cumulative weight distribution plots (Fig. 9). RT-8, also a beta-glucan sample from oat, showed the least difference in the MMD profile between Labs 5 and 6 (Fig. 9). Replicate measurements (n = 3) of samples were less variable for the purer beta-glucan samples than for those that contained less BG but higher M's (Table 2B).

4. Discussion

It would appear that molecular dissolved BG in typical dilute solution conditions dominate during the SEC-based analysis methods (DMAc/LiCl and aqueous mobile phases), capillary viscometry, SV-AUC, and to a large extent, one of the AF4 based methods (Lab 5). All these methods arrive at similar M_w's for the three purest of the six BG isolates, while for the samples containing less pure BG isolates the determined M_w values were more variable between methods. As observed in an earlier study (Rieder et al., 2015) calcofluor detection underestimates the samples with the highest M_w. In terms of variability between replicate measurements, it was quite low for methods where duplicate measurements were made immediately on the same day except for capillary viscometry for a couple of samples. For SEC-MALS-VISC-RI, which included a dataset collected over a 5-month interval, reproducibility was reassuringly good for the pure samples with the highest BG content. However, for the samples with higher BG M_w, and lower BG content due to the presence of impurities, the difference between the highest and lowest M_w values was as much as 25%. This may represent longer-term changes in conditions in the SEC and detector system and/or changes in the samples themselves.

It is mostly *M* values for BG analysed by these methods, in particular the aqueous-SEC based methods with post-column calcofluor detection, that have been found to correlate with health benefits of beta-glucan containing foods such as reduced fasting LDL-cholesterol levels in the blood (Wang et al., 2016; Wolever et al., 2010a) or reduced

post-prandial glycaemic responses (Brummer et al., 2012; Regand et al., 2009; Rieder et al., 2017; Tosh, 2013; Tosh et al., 2008; Wolever et al., 2019). Molecular weight (*M*) or equivalent term molar mass, is an exclusive fundamental property of non-interacting molecules and is probably one of the most important parameters defining a macromolecule. It is the molecular weight characteristics of individual dissolved BG, as extracted from a foods or grain ingredients containing BG, that has been correlated with physiological and clinical outcomes. However, the impact of BG aggregates and supramolecular structures for *in vivo* effects is poorly understood. If M_w values for BG correlate well with clinical outcomes, it might be intuitive to assume that because the calculated M_w values are significantly biased to higher values because of chain aggregation, these will have little or no correlation to the same clinical outcomes. After all, the size of aggregates in analytical measurements must also be a function of their concentration, the solute composition, and other factors such as solvent properties. However, whether aggregates contribute to the overall rheological properties of BG, or whether they have a physiological relevance through interaction with enzymes, substrates or mucus is currently not known.

Nevertheless, the results of a study in pigs suggest that solubilised oat BG (presumably present as individual chains in solution) can decrease the permeability of *ex-vivo* mucus to nutrients (Mackie et al., 2016). Populations of molecular aggregates/supramolecular aggregates were of abundance, at least in certain samples, analysed by the AF4 method used by Lab 6. Generally, these samples also had the largest M_w among the methods we evaluated. During the previous decade other studies using the same type of AF4 system (Wyatt) have observed similar results (Håkansson et al., 2012; Zielke, Stradner, & Nilsson, 2018). Several types of aggregate species of BG have been noted in previous work including fringed micelles, swollen microgels and secondary 'aggregates of aggregates' (Grimm et al., 1995; Zielke, Stradner, & Nilsson, 2018). It is quite likely that all these structures are present in solution preparations of the samples tested in the current study. Molecularly dissolved species are likely also present (Zielke, Stradner, & Nilsson, 2018), yet in other samples of BG their absence has been noted (Korompokis et al., 2018).

In a recent study of the same BG material used to prepare RT-8 (>90% BG), AF4 analysis demonstrated that calculated *M*-distribution displayed a large range from 10^5 to 5×10^7 g/mol (Zielke, Lu, Poinsot, & Nilsson, 2018) with a peak *M* around 8×10^5. No value for M_w was calculated. Based on the low <0.7 ratio of r_{rms}/r_{hyd} (Zielke, Lu, et al., 2018), a microgel structure for the entire sample distribution was proposed.

Clear differences in BG *M* determinations between the two types of AF4 system studied here have also been noted before (Mäkelä et al., 2015). Differences in sample preparation were proposed as an explanation (Mäkelä et al., 2015). Under milder dissolution conditions (70 °C, 30 min) it was suggested that aggregates (presumably not fully dissolved) could dominate, while under slightly harsher conditions with adequate heating (85 °C, 2h) aggregation of BG is minimised (Mäkelä et al., 2015). The results from our current study point strongly to another explanation since all assessed aqueous BG samples had an identical dissolution history. Each laboratory was also given strict instructions to place each sample in a boiling water bath for 5 min, but not to filter prior to analysis. It is also known that treatments such as heating to 90 °C, filtration, urea, and sonication cannot completely eliminate aggregates of BG in dilute aqueous solution (Li et al., 2006). Rapid molecular re-association occurs through inter-molecular hydrogen bonding once the treatment is reversed (Li et al., 2006, 2011). Indeed, aqueous solutions are poor solvents for many polysaccharides including cereal BG. It would seem there are differences in operating conditions between the whole or parts of the two AF4 systems used by Labs 5 and 6. The system used by Lab 5 could be subjected in some part to larger shearing forces, than that used by Lab 6, shifting the equilibrium of molecular association-dissociation to strongly favour dissociation. Detailed differences in operating conditions between the two systems, however, were not investigated. The more dilute salt concentration used in the carrier phase (10 mM) by Lab 6 compared to Lab 5 (100 mM) is not expected to explain the difference in molecular/aggregate species since BG aggregation has previously been observed in 0.1 M NaCl (Vårum et al., 1992).

Beta-glucan aggregates seem to be disrupted by applying a low shearing force. Chain-scission by shearing forces has also been observed for other types of polymers such as starch amylopectin during SEC with molecules of *M* 's > 10^6 g/mol being particularly susceptible (Barth & Carlin, 1984; Cave et al., 2009). Whether chain-scission occurs in the current study during SEC-analysis is not definitively known but given that several different methods, including analytical ultracentrifugation, returned similar results for all samples it would seem unlikely. Furthermore, BG subjected to shear rates from 0.1 to 500 s^{-1} in a rheometer had a generally overlaid viscosity profile of forward and backward ramps (Rieder et al., 2017). This demonstrates a general stability and lack of chain scission under such shearing conditions. Nevertheless, macromolecules subjected to SV-AUC are subjected to hydrostatic pressures. In the Beckman Ultima centrifuge employing a AN60Ti rotor with 12 mm path lengths, average pressures of around 75 bar were estimated at a rotor speed of 40000 rpm (Stoutjesdyk, Brookes, Henrickson, & Demeler, 2020). Similar pressures are likely in our system and are perhaps enough to favour the dissociated molecularly dissolved state of BG. For oligomeric proteins, hydrostatic pressures of 1–3 kbar are needed for full dissociation, which is often reversible and without denaturation (Gorovits, Raman, & Horowitz, 1995). One would expect large supramolecular aggregates to precipitate in the high speed ultracentrifuge (Gillis, Rowe, Adams, & Harding, 2014) but of course only if they remain intact and do not dissociate first.

It is currently debated whether dissolution of BG in sodium hydroxide can dissolve aggregates or not (Håkansson et al., 2012; Li et al., 2011). A mixture of DMAc/9% LiCl is a common organic solvent-salt mixture used to molecularly dissolve cellulose by disruption of hydrogen bonds to thus minimise interactions between molecules (Potthast et al., 2015). It should also be expected that this solvent, like traditional cellulose solvents such as cuoxam, will molecularly dissolve BG and readily abolish aggregates (Grimm et al., 1995). Further, in-line with observations in this study it has previously been noted that DMAc/LiCl, compared to aqueous solvents and mobile phases, returned similar results for M_w of BG when analysed using SEC-MALS (Kivelä, Henniges, Sontag-Strohm, & Potthast, 2012).

MHKS-exponents of 0.5–0.6 in aqueous SEC-MALS-VISC-RI are also in line with the random coil conformation, again consistent with molecularly dissolved species under the conditions of such analysis. This is further supported by the observation that BG evaluated by capillary viscometry or SEC, which seems to strongly favour dissociation into single molecules, exhibit flow behaviour typical of other random coil biopolymers, where once the entanglement concentration is reached the solutions depart from Newtonian behaviour (Morris, 1989). From SV-AUC experiments, extrapolation of the sedimentation coefficient against concentration yields the Gralén coefficient (k_s) (Gralén, 1944). Combined with the intrinsic viscosity (Wales–Van Holde ratio, $k_s/[\eta]$), it gives an indication of the shape of the macromolecule (Creeth & Knight, 1965; Wales et al., 1954). Thus, for a perfect sphere or non-draining random coil $k_s/[\eta] = 1.6$, whereas lower values represent macromolecules with asymmetry. The $k_s/[\eta]$ values in this study of 1.4–1.6 again point towards a random coil conformation i.e., molecularly dissolved species in sedimentation velocity, and not aggregates (Creeth and Knight, 1965).

Both SV-AUC and capillary viscometry rely on *a priori* knowledge of the power law parameters *b* and κ_s and *a* and *k,* respectively, to calculate M_w. However, both these techniques are still absolute methods, and neither require calibration standards, nor assumptions on conformation. Since values for these power law parameters have been obtained from SEC-MALS-VISC-RI for this study it is not surprising they should correlate well with our aqueous SEC-data. Sedimentation equilibrium

analytical ultracentrifugation is the sister technique to SV. It has previously been used to determine M_w including that of BG (Woodward et al., 1983), but its main disadvantage is the excessive long run times (days) often required to reach equilibrium.

Three of our samples contained thermally denatured oat/barley protein co-extracted with the BG, and probably also remnants of non-denatured thermostable alpha-amylase. The same three samples also contained small amounts of arabinoxylan. Starch degradation products were absent since these were washed out by repeated ethanol washes during beta-glucan preparation. In previously unpublished work using preparative SEC (Sephacryl 200) with a sample similar to RT-7 extracted from Swedish Oatfiber - Oatwell 28, we found the protein fraction to be of small *M* and completely separated from the larger BG fraction (result not shown). This provides further evidence to suggest that it was M_w of BG that were measured in the current study and not that of protein. Recovery results from Lab 6 also support the contention that during measurement, protein is not bound to BG. For electrostatic interactions to occur between oat BG that may contain phosphate and protein in solution, the pH must be < 4 and at low ionic strength (Zielke, Lu, et al., 2018).

So long as there is an absence of di/trivalent metal ions and no beta-glucanase activity then dilute solutions of BG seem to be stable during prolonged cold storage in the dark. Given that BG are difficult to get into aqueous solution and they can easily be depolymerised during dissolution e.g., via beta-glucanase contamination, their dissolution can be difficult to reproduce from one laboratory to another. Perhaps commercial suppliers should consider producing well-characterised BG solutions for sale as *M* standards rather than dried/freeze dried powders?

In conclusion, the SEC, viscometry, and SV-AUC methods all produced M_w values seemingly based on individual dissolved BG molecules, while certain AF4 systems measured molecular aggregates or supramolecular aggregates in addition to individual dissolved molecules. Calculation of M_w for the latter system, including these aggregates, results in much higher M_w values because M_w is defined strictly as the weight of individual non-interacting molecules in units of g/mol. These M_w values containing aggregates have so far not been correlated with the *in vivo* effects of BG, which may indeed be difficult as the size of aggregates in analytical measurements must also be a function of their concentration, the solute composition, and other factors. However, as newer methods like AF4 become more widely available, aggregating properties of BG and their potential impact on physiological outcomes should be further investigated. Amongst the methods measuring individually dissolved molecules of BG, the calcofluor method deviated the most from the others and resulted in an underestimation of M_w for two of the beta-glucan extracts containing the largest molecularly dissolved species. It is, however, the only method that does not require 'purified' extracts of BG and thus will remain useful to estimate M_w and the extent of beta-glucan degradation in processed foods if calibrated correctly using high M_w standards. For in-house ingredient quality evaluation of BG in the food industry, perhaps the easiest and cheapest way to evaluate M_w is indirectly via measuring $[\eta]_w$ with no practical need to even convert it to M_w. For measurements in the analytical laboratory, then the SEC-MALS methods are probably the current method of choice, especially if they can be combined with a suitable extraction and purification procedure to enable determination of BG M_w in processed foods. Better characterisation of *M* of BG for physiological and nutritional studies is an important task for the future, including reliable estimates of molecular weight of solubilised BG as well as aggregation properties. Current labels on food packaging only provide information on the dietary fibre content. In the future, additional food label information might include quantitative data about dietary fibre quality (Augustin et al., 2020). This could include the type of dietary fibre present and a measure of its weight-average molecular weight.

Declaration of interest

Declarations of interest: none.

CRediT author statement

Simon Ballance: Conceptualization, Validation, Investigation, Writing - Original Draft, Writing - Review & Editing, Visualization, Project administration, **Yudong Lu:** Investigation, **Hanne Zobel:** Investigation, **Anne Rieder:** Validation, Investigation, Writing - Review & Editing, **Svein Halvor Knutsen:** Investigation, Writing - Review & Editing, **Vlad T Dinu:** Investigation, **Bjørn E. Christensen:** Validation, Investigation, Writing - Review & Editing, **Ann-Sissel Ulset:** Investigation, **Marius Schmid:** Validation, Investigation, Writing - Review & Editing, **Ndegwa Maina:** Validation, Investigation, Writing - Review & Editing, **Antje Potthast:** Validation, Investigation, Writing - Review & Editing, **Sonja Schiehser:** Investigation, **Peter R. Ellis:** Conceptualization, Validation, Writing - Review & Editing, **Stephen E. Harding:** Conceptualization, Validation, Investigation, Writing - Review & Editing.

Declaration of interests

The authors declare that they have no known competing financial interests or personal relationships that could have appeared to influence the work reported in this paper.

Acknowledgments

SB, SKN, HZ and AR thank the Norwegian Fund for Research Fees for Agricultural Products (FFL) for supporting the study through the project "SusHealth" (project number 314599). SHE, VTD and PRE were funded by the BBSRC DRINC project BB/L025272/1 (United Kingdom).

Appendix A. Supplementary data

Supplementary data to this article can be found online at https://doi.org/10.1016/j.foodhyd.2022.107510.

References

Augustin, L. S. A., Aas, A.-M., Astrup, A., Atkinson, F. S., Baer-Sinnott, S., Barclay, A. W., et al. (2020). Dietary fibre consensus from the international carbohydrate quality consortium (ICQC). *Nutrients, 12*(9), 2553.

Barth, H., & Carlin, F., Jr. (1984). A review of polymer shear degradation in size-exclusion chromatography. *Journal of liquid chromatography, 7*(9), 1717–1738.

Brummer, Y., Duss, R., Wolever, T. M. S., & Tosh, S. M. (2012). Glycemic response to extruded oat bran cereals processed to vary in molecular weight. *Cereal Chemistry, 89*(5), 255–261.

Cave, R. A., Seabrook, S. A., Gidley, M. J., & Gilbert, R. G. (2009). Characterization of starch by size-exclusion chromatography: The limitations imposed by shear scission. *Biomacromolecules, 10*(8), 2245–2253.

Channell, G. A., Adams, G. G., Lu, Y., Gillis, R. B., Dinu, V., Grundy, M. M.-L., et al. (2018). Use of the Extended Fujita method for representing the molecular weight and molecular weight distributions of native and processed oat beta-glucans. *Scientific Reports, 8*(1), 1–8.

Christensen, B. E., Ulset, A. S., Beer, M. U., Knuckles, B. E., Williams, D. L., Fishman, M. L., et al. (2001). Macromolecular characterisation of three barley β-glucan standards by size-exclusion chromatography combined with light scattering and viscometry: An inter-laboratory study. *Carbohydrate Polymers, 45*, 11–22.

Creeth, J., & Knight, C. (1965). On the estimation of the shape of macromolecules from sedimentation and viscosity measurements. *Biochimica et Biophysica Acta (BBA)-Biophysics including Photosynthesis, 102*(2), 549–558.

Dam, J., & Schuck, P. (2004). Calculating sedimentation coefficient distributions by direct modeling of sedimentation velocity concentration profiles. *Methods in Enzymology, 384*, 185–212.

EFSA. (2010). Scientific Opinion on the substantiation of a health claim related to oat beta-glucan and lowering blood cholesterol and reduced risk of (coronary) heart disease pursuant to Article 14 of Regulation (EC) No 1924/2006. *EFSA Journal*, (8).

EFSA. (2011a). Scientific Opinion on the substantiation of a health claim related to barley beta-glucans and lowering of blood cholesterol and reduced risk of (coronary) heart disease pursuant to Article 14 of Regulation (EC) No 1924/2006. *EFSA Journal*, (9).

EFSA. (2011b). Scientific Opinion on the substantiation of health claims related to beta-glucans from oats and barley and maintenance of normal blood LDL-cholesterol concentrations (ID 1236, 1299), increase satiety leading to a reduction in energy intake (ID 851, 852), reduction of post-prandial glycaemic responses (ID 821, 824), and "digestive function" (ID 850) pursuant to Article 13(1) of Regulation (EC) No 1924/2006. *EFSA Journal*, (9).

Englyst, H. N., Quigley, M. E., & Hudson, G. J. (1994). Determination of dietary fiber as non-starch polysaccharides with gas-liquid-chromatographic, high-performance liquid-chromatographic or spectrophotometric measurement of consitituent sugars. *Analyst, 119*(7), 1497–1509.

Folch, J., Lees, M., & Stanley, G. S. (1957). A simple method for the isolation and purification of total lipides from animal tissues. *Journal of Biological Chemistry, 226*(1), 497–509.

Gillis, R. B., Rowe, A. J., Adams, G. G., & Harding, S. E. (2014). A review of modern approaches to the hydrodynamic characterisation of polydisperse macromolecular systems in biotechnology. *Biotechnology & Genetic Engineering Reviews, 30*(2), 142–157.

Gómez, C., Navarro, A., Manzanares, P., Horta, A., & Carbonell, J. V. (1997). Physical and structural properties of barley (1 → 3),(1 →4)-β-D-glucan. Part I. Determination of molecular weight and macromolecular radius by light scattering. *Carbohydrate Polymers, 32*, 7–15.

Gorovits, B., Raman, C., & Horowitz, P. M. (1995). High hydrostatic pressure induces the dissociation of cpn60 tetradecamers and reveals a plasticity of the monomers. *Journal of Biological Chemistry, 270*(5), 2061–2066.

Gralén, N. (1944). *Sedimentation and diffusion measurements on cellulose and cellulose derivatives*. Unpublished PhD, University of Uppsalla.

Green, A. A. (1933). The preparation of acetate and phosphate buffer solutions of known pH and ionic strength. *Journal of the American Chemical Society, 55*(6), 2331–2336.

Grimm, A., Krüger, E., & Burchard, W. (1995). Solution properties of β-D-(1, 3)(1, 4)-glucan isolated from beer. *Carbohydrate Polymers, 27*, 205–214.

Grundy, M. M.-L., Quint, J., Rieder, A., Ballance, S., Dreiss, C. A., Butterworth, P. J., et al. (2017). Impact of hydrothermal and mechanical processing on dissolution kinetics and rheology of oat β-glucan. *Carbohydrate Polymers, 166*, 387–397.

Håkansson, A., Ulmius, M., & Nilsson, L. (2012). Asymmetrical flow field-flow fractionation enables the characterization of molecular and supramolecular properties of cereal β-glucan dispersions. *Carbohydrate Polymers, 87*(1), 518–523.

Harding, S. E. (1992). Sedimentation analysis of polysaccharides. In S. E. Harding, A. J. Rowe, & J. Horton (Eds.), *Analytical ultracentrifugation in biochemistry and polymer science* (pp. 495–516). Cambridge: Royal Society of Chemistry.

Harding, S. E., Schuck, P., Abdelhameed, A. S., Adams, G., Kök, M. S., & Morris, G. A. (2011). Extended Fujita approach to the molecular weight distribution of polysaccharides and other polymeric systems. *Methods, 54*(1), 136–144.

Jin, Y.-L., Speers, R. A., Paulson, A. T., & Stewart, R. J. (2004). Barley beta-glucans and their degradation during malting and brewing. *Technical Quarterly - Master Brewers Association of the Americas, 41*(3), 231–240.

Kivelä, R., Henniges, U., Sontag-Strohm, T., & Potthast, A. (2012). Oxidation of oat β-glucan in aqueous solutions during processing. *Carbohydrate Polymers, 87*(1), 589–597.

Korompokis, K., Nilsson, L., & Zielke, C. (2018). The effect of in vitro gastrointestinal conditions on the structure and conformation of oat β-glucan. *Food Hydrocolloids, 77*, 659–668.

Lazaridou, A., Biliaderis, C. G., & Izydorczyk, M. S. (2007). Cereal beta-glucans: Structures, physical properties, and physiological functions. In C. G. Biliaderis, & M. S. Izydorczyk (Eds.), *Functional food carbohydrates* (pp. 1–72). Boca Raton: CRC Press.

Li, W., Cui, S., Wang, Q., & Yada, R. (2011). Studies of aggregation behaviours of cereal β-glucans in dilute aqueous solutions by light scattering: Part I. Structure effects. *Food Hydrocolloids, 25*(2), 189–195.

Li, W., Wang, Q., Cui, S., Huang, X., & Kakuda, Y. (2006). Elimination of aggregates of (1→ 3)(1→ 4)-β-D-glucan in dilute solutions for light scattering and size exclusion chromatography study. *Food Hydrocolloids, 20*(2–3), 361–368.

Mackie, A., Rigby, N., Harvey, P., & Bajka, B. (2016). Increasing dietary oat fibre decreases the permeability of intestinal mucus. *Journal of Functional Foods, 26*, 418–427.

Mäkelä, N., Sontag-Strohm, T., & Maina, N. H. (2015). The oxidative degradation of barley β-glucan in the presence of ascorbic acid or hydrogen peroxide. *Carbohydrate Polymers, 123*, 390–395.

Morris, E. R. (1989). Polysaccharide solution properties: Origin, rheological characterization and implications for food systems. In R. P. Millane, & J. N. BeMiller (Eds.), *Frontiers in carbohydrate Research I. Food applications* (pp. 132–162). New York: Elsevier.

Nilsson, L. (2013). Separation and characterization of food macromolecules using field-flow fractionation: A review. *Food Hydrocolloids, 30*(1), 1–11.

Potthast, A., Radosta, S., Saake, B., Lebioda, S., Heinze, T., Henniges, U., et al. (2015). Comparison testing of methods for gel permeation chromatography of cellulose: Coming closer to a standard protocol. *Cellulose, 22*(3), 1591–1613.

Regand, A., Tosh, S. M., Wolever, T. M. S., & Wood, P. J. (2009). Physicochemical properties of beta-glucan in differently processed oat foods influence glycemic response. *Journal of Agricultural and Food Chemistry, 57*(19), 8831–8838.

Rieder, A., Knutsen, S. H., & Ballance, S. (2017). In vitro digestion of beta-glucan rich cereal products results in extracts with physicochemical and rheological behavior like pure beta-glucan solutions–A basis for increased understanding of in vivo effects. *Food Hydrocolloids, 67*, 74–84.

Rieder, A., Knutsen, S. H., Ulset, A.-S. T., Christensen, B. E., Andersson, R., Mikkelson, A., et al. (2015). Inter-laboratory evaluation of SEC-post-column calcofluor for determination of the weight-average molar mass of cereal β-glucan. *Carbohydrate Polymers, 124*, 254–264.

Rimsten, L., Stenberg, T., Andersson, R., Andersson, A., & Åman, P. (2003). Determination of β-Glucan molecular weight using SEC with calcofluor detection in cereal extracts. *Cereal Chemistry, 80*, 485–490.

Stoutjesdyk, M., Brookes, E., Henrickson, A., & Demeler, B. (2020). Measuring compressibility in the optima AUC™ analytical ultracentrifuge. *European Biophysics Journal, 49*(8), 711–718.

Thondre, P., Shafat, A., & Clegg, M. (2013). Molecular weight of barley β-glucan influences energy expenditure, gastric emptying and glycaemic response in human subjects. *British Journal of Nutrition, 110*(12), 2173–2179.

Tosh, S. M. (2013). Review of human studies investigating the post-prandial blood-glucose lowering ability of oat and barley food products. *European Journal of Clinical Nutrition, 67*(4), 310–317.

Tosh, S. M., Brummer, Y., Wolever, T. M. S., & Wood, P. J. (2008). Glycemic response to oat bran muffins treated to vary molecular weight of beta-glucan. *Cereal Chemistry, 85*(2), 211–217.

Ulmius, M., Önning, G., & Nilsson, L. (2012). Solution behavior of barley β-glucan as studied with asymmetrical flow field-flow fractionation. *Food Hydrocolloids, 26*, 175–180.

Vårum, K. M., & Smidsrød, O. (1988). Partial chemical and physical characterisation of (1→ 3),(1→ 4)-β-D-glucans from oat (Avena sativa L.) aleurone. *Carbohydrate Polymers, 9*(2), 103–117.

Vårum, K. M., Smidsrød, O., & Brant, D. A. (1992). Light scattering reveals micelle-like aggregation in the (1→ 3),(1→ 4)-β-D-glucans from oat aleurone. *Food Hydrocolloids, 5*, 497–511.

Wales, M., & Van Holde, K. (1954). The concentration dependence of the sedimentation constants of flexible macromolecules. *Journal of Polymer Science, 14*(73), 81–86.

Wang, Q., & Ellis, P. R. (2014). Oat β-glucan: Physico-chemical characteristics in relation to its blood-glucose and cholesterol-lowering properties. *British Journal of Nutrition, 112*(S2), S4–S13.

Wang, Y. N., Harding, S., Eck, P., Thandapilly, S. J., Gamel, T. H., Abdel-Aal, E.-S. M., et al. (2015). High-molecular-weight β-glucan decreases serum cholesterol differentially based on the CYP7A1 rs3808607 polymorphism in mildly hypercholesterolemic adults. *Journal of Nutrition, 146*(4), 720–727.

Wang, Y. N., Harding, S. V., Eck, P., Thandapilly, S. J., Gamel, T. H., Abdel-Aal, E. S. M., et al. (2016). High-molecular-weight beta-glucan decreases serum cholesterol differentially based on the CYP7A1 rs3808607 polymorphism in mildly hypercholesterolemic adults. *Journal of Nutrition, 146*(4), 720–727.

Wang, Q., Wood, P., & Cui, W. (2002). Microwave assisted dissolution of β-glucan in water—implications for the characterisation of this polymer. *Carbohydrate Polymers, 47*(1), 35–38.

Wolever, T. M. S., Tosh, S. M., Gibbs, A. L., Brand-Miller, J., Duncan, A. M., Hart, V., et al. (2010a). Physicochemical properties of oat beta-glucan influence its ability to reduce serum LDL cholesterol in humans: A randomized clinical trial. *American Journal of Clinical Nutrition, 92*(4), 723–732.

Wolever, T. M. S., Tosh, S. M., Gibbs, A. L., Brand-Miller, J., Duncan, A. M., Hart, V., et al. (2010b). Physicochemical properties of oat β-glucan influence its ability to reduce serum LDL cholesterol in humans: A randomized clinical trial. *American Journal of Clinical Nutrition, 92*(4), 723–732.

Wolever, T. M. S., Tosh, S. M., Spruill, S. E., Jenkins, A. L., Ezatagha, A., Duss, R., et al. (2019). Increasing oat β-glucan viscosity in a breakfast meal slows gastric emptying and reduces glycemic and insulinemic responses but has no effect on appetite, food intake, or plasma ghrelin and PYY responses in healthy humans: A randomized, placebo-controlled, crossover trial. *The American Journal of Clinical Nutrition, 111*(2), 319–328.

Woodward, J., Phillips, D., & Fincher, G. (1983). Water-soluble (1→ 3),(1→ 4)-β-D-glucans from barley (Hordeum vulgare) endosperm. I. Physicochemical properties. *Carbohydrate Polymers, 3*(2), 143–156.

Xiao, X., Tan, C., Sun, X., Zhao, Y., Zhang, J., Zhu, Y., et al. (2020). Effects of fermentation on structural characteristics and in vitro physiological activities of barley β-glucan. *Carbohydrate Polymers, 231*, Article 115685.

Zielke, C., Lu, Y., Poinsot, R., & Nilsson, L. (2018). Interaction between cereal β-glucan and proteins in solution and at interfaces. *Colloids and Surfaces B: Biointerfaces, 162*, 256–264.

Zielke, C., Stradner, A., & Nilsson, L. (2018). Characterization of cereal β-glucan extracts: Conformation and structural aspects. *Food Hydrocolloids, 79*, 218–227.